EVAPORATING COOLANT FOR ON-BOARD COOLING SYSTEMS WITH DIRECT CONDENSATION THROUGH AMBIENT AIR

S. Adeyefa, F. Thielecke, U. Carl
Institute of Aircraft Systems Engineering, Hamburg University of Technology (TUHH), Germany

Keywords: *Carbon dioxide, cooling system, evaporating coolant*

Abstract

On-board cooling systems using carbon dioxide are of interest due to possible advantages in installation space and system mass. Here, a new system architecture is introduced using CO_2 as an evaporating coolant in a secondary distribution cycle condensed by a primary vapour cycle for ground operations and by ambient air during flight. Deactivation of active vapour cycle cooling enables benefits regarding power consumption and availability.
Experimental investigations regarding ground operation at high ambient temperatures are discussed outlining the evaporating coolant cycle characteristics. Based on the derived system behaviour and relevant boundary conditions, a simulation model of the ambient heat exchanger is used to determine the performance envelope and feasibility of direct condensation, based on an automotive heat exchanger without optimisation for the intended application.

1 Introduction

On-board cooling systems supplying cooling capacity for commercial and electrical power consumers, are dealing with rising heat loads as progressive electrification of future aircraft takes place. For the resulting More- or All-Electric-Aircraft, minimisation of system mass and power consumption is a design driver regarding the cooling system to retain an overall benefit. In addition, tendencies to rising power and thus waste heat flux densities account for new cooling solutions. Optimisation of cooling performance and power consumption can be achieved by improving the heat exchange at both heat rejection and absorption through employing phase changing (2-phase), contrary to currently used liquid (single phase) working fluids.

In previous investigations, a direct expansion system approach has been investigated as cold generation for aircraft air conditioning [5] and equipment cooling with multiple parallel consumers [2], [9]. As stated in [2], reductions in system mass can be realised using the low global warming potential fluid carbon dioxide, which is currently of high and rising interest for European car manufacturers due to changes concerning regulations on mobile cooling systems [7]. As a matter of principle, efficiencies are superior to systems involving a secondary liquid coolant to distribute cooling capacity along the aircraft due to direct heat transfer, also rendering additional pumping power unnecessary. On the other hand, introducing carbon dioxide (CO_2) as working fluid in a vapour cycle is linked to pressures over 90 bar when used at ambient temperatures over 30 °C, leading to higher safety risks regarding component failure effects on equipment and humans inside the cabin.

As a baseline for the following investigations, representing a compromise between lower safety risks and high heat transfer rates, a secondary coolant loop was implemented into an existing

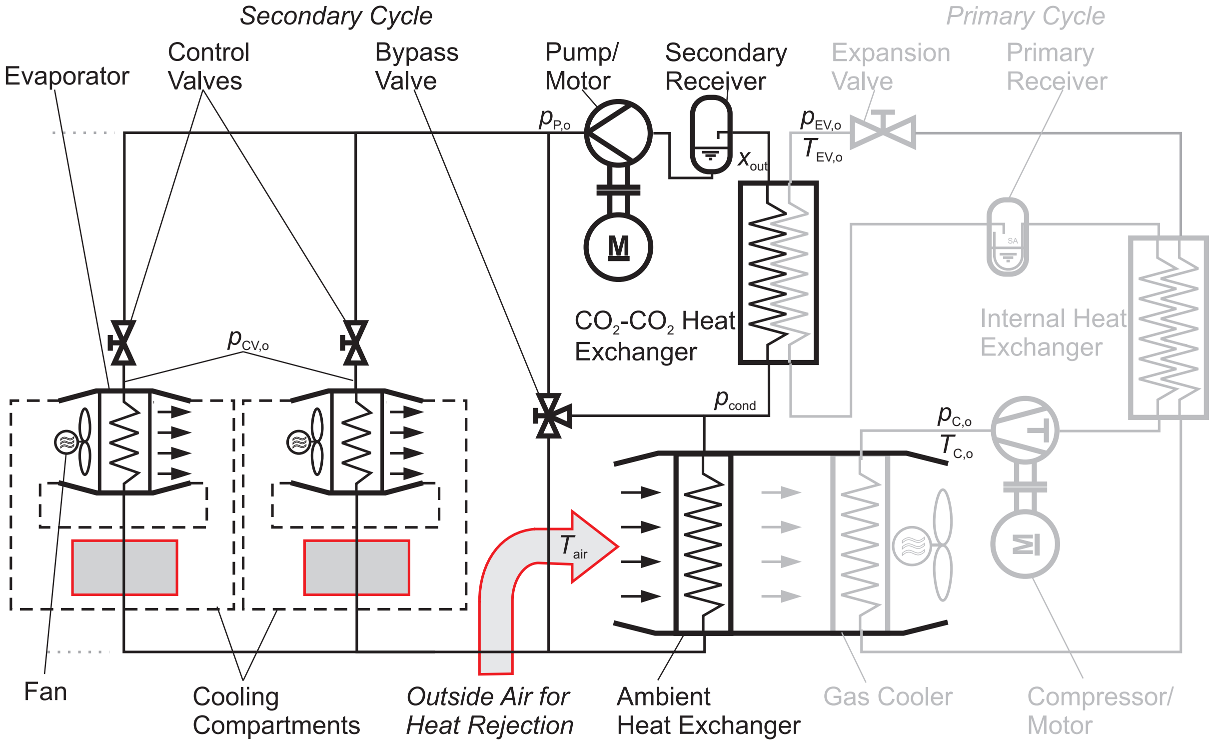

Fig. 1 Cooling System Scheme with Primary Vapour Cycle and Secondary Evaporating Coolant Cycle

CO_2 cooling system, in which an evaporating coolant - CO_2 in this case - is circulated. Thus, the high pressures of the cold generation unit are locally isolated.
Based on the system described in the following, the main operating modes, which are the ground and flight case, are investigated using both experimental and numerical methods.

Since aircraft cooling systems are exposed to a wide range of boundary conditions, especially if outboard air is used for heat rejection, the outside air temperatures during cruise ($T_{ISA}|_{37\,\mathrm{kft}} = -54$ °C) are well below the cooling point temperatures ($T_{dem} = -1 \ldots 20$ °C). Thus, the power put into a refrigeration process could be saved and only the secondary cycle remains active. Figure 2 displays the flight envelope over time for a short range aircraft with outside air temperature according to ISA. It can be observed, that the calculated ram air temperature under consideration of maximum temperature recovery shows a significant temperature difference during most of the flight time. Using condensation heat exchange as

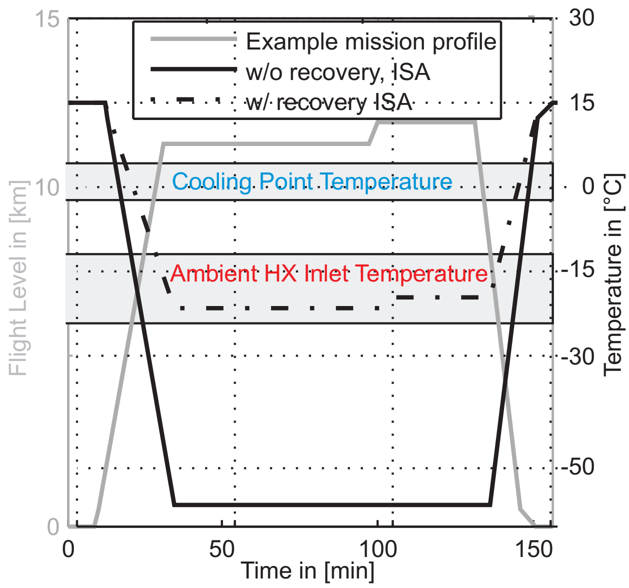

Fig. 2 Boundary conditions for on-board cooling system with ambient air heat rejection

for the introduced 2-phase coolant, this temperature difference can be utilised directly with low ram air flows ($\dot{m}_{Air} \leq 0.4$ kg/s for targeted cooling capacity) and compact heat exchanger geometry.

2 Evaporating Coolant System architecture

The derived system architecture for on-board cooling using CO_2 in two interchanging cycles connected by a CO_2-CO_2 heat exchanger is shown schematically in Fig. 1.

2.1 Process description

While in this paper, emphasis shall be put on the secondary cycle, both sides of the system are briefly described as follows:

Primary Cycle - Cold Generation

For ground operation, a conventional CO_2 vapour cycle with a suction side Receiver and an Internal Heat Exchanger is used for cold generation in a mostly transcritical refrigeration process, meaning heat is rejected at a pressure and temperature above the critical point ($T_{crit} = 31.0$ °C, $p_{crit} = 73.8$ bar). The gaseous refrigerant exits the compressor with high pressure ($p_{C,o} \approx 80\ldots110$ bar) and high temperature ($T_{C,o} \approx 110\ldots170$ °C), and is then cooled in the Gas Cooler and Internal Heat Exchanger (IHX). An Expansion Valve reduces both pressure ($p_{EV,o} \approx 17\ldots30$ bar) and temperature ($T_{EV,o} \approx -25\ldots-5$ °C). The evaporating refrigerant absorbs heat in the CO_2-CO_2 heat exchanger and enters the Receiver where refrigerant is accumulated and liquid is separated from gas before both fractions reenter the IHX.

Secondary Cycle - Coolant Distribution

Liquid coolant enters the pump and is discharged into a centralised coolant bus, to supply the consumers at a pressure of $p_{P,o} \approx 32\ldots45$ bar. The flow through the evaporator of each cooling point is controlled by a valve, which causes only minor expansion ($p_{CV,o} \approx 30\ldots45$ bar) defining the corresponding evaporation temperature. A joint merges fluid bypassed and from the evaporators to the total coolant mass flow passing the CO_2-CO_2 heat exchanger where a low exit vapour quality ($x = 0\ldots0.2$) is required to avoid cavitation in the pump. This is supported by the Secondary Receiver separating gas from liquid phase and providing the latter to the pump.

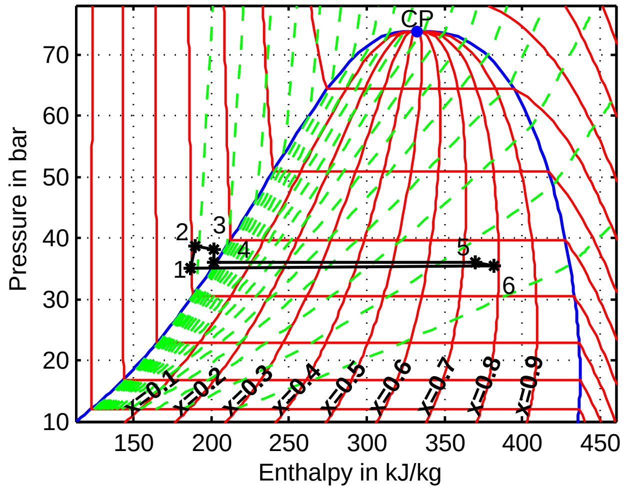

Fig. 3 Example for secondary cycle process in *p*-*h*-diagram for CO_2

A simplified example process of the secondary CO_2 coolant distribution cycle is shown in Fig. 3 with state changes as follows:

1. $\rightarrow$ 2.: liquid CO_2 discharged by pump
2. $\rightarrow$ 3.: transport via supply line
3. $\rightarrow$ 4.: pressure drop at control valve
4. $\rightarrow$ 5.: heat exchange at evaporator
5. $\rightarrow$ 6.: transport via return line
6. $\rightarrow$ 1.: condensation at the CO_2-CO_2 Heat Exchanger or Ambient HX respectively

2.2 Cooling System Test Rig

In order to demonstrate the capabilities of an evaporating coolant system architecture, an existing test rig for direct evaporation with multiple consumers, as discussed in [2], was modified and expanded according to Fig. 1, less the Ambient Heat Exchanger (AHX). All included components are automotive, prototype or industrial type neither airworthy components nor optimised for the specific application leading to certain constraints regarding efficiency and performance. However, the test rig allows for experimental investigations regarding potentials of utilising CO_2 as an evaporating coolant. It should be stated, that the AHX is not yet integrated into the experimental system.

Regarding Fig. 3 it can be observed, that condensation and evaporation take place at approximately equal pressure levels. In combination with low mass flow rates, minimal pumping power is required. A 5-stage centrifugal pump, designed as a hermetic canned motor-pump, is used to circulate the coolant in the secondary loop. The canned motor allows hydrodynamic bearing of the rotor, without an additional lubricant as required for compressors. This renders complex lubricant separation and return causing pressure loss unnecessary. Pump and motor are passed through by CO_2 partially evaporating due to heat gain. For the specific application of pumping liquid CO_2, the inlet and outlet of the pump are coaxial (inlet $\rightarrow$ centrifugal pump, motor $\rightarrow$ outlet). Since evaporation is part of the pump unit operation method, a minor vapour quality, defined as

$$x = \frac{m_{vapour}}{m_{liquid} + m_{vapour}} \in [0;1] \tag{1}$$

in the pump supply line is tolerable, though it has to be limited to $x \approx 0.2$ by adequate condensation.
The Secondary Receiver is used to ensure a reservoir of liquid coolant at the pump inlet during critical transients (e.g. rising heat loads). Its volume is explicitly oversized ($V_R = 1.3$ l) for laboratory operation and can be reduced or completely eliminated for the very application.
The turbo-machine regarded for laboratory testing requires a minimum flow under all operating conditions which is not reached with supply of the consumer stations only. To allow a sufficient flow rate, also decreasing the inlet vapour quality to the CO_2-CO_2 Heat Exchanger (or AHX, respectively), a bypass line connects the pump outlet and the CO_2-CO_2 Heat Exchanger inlet (and/or AHX outlet). A manual bypass valve operates as a nozzle to adjust a nominal flow which could also be electrically driven to utilise it as an additional actuating element.

2.3 System dimensions

Relative position of the cooling generation plant and the consumers define the system volume and thus, in combination with the operating range, refrigerant/coolant charge of the high volumetric cooling capacity fluid CO_2. In Tab. 4, the resulting parameters of the defined test rig setup are listed.

	diam.	length	
supply line E1	3/8"	7.61	m
return line E1	1/2"	8.80	m
supply line E2	3/8"	3.10	m
return line E2	1/2"	3.18	m
internal piping		5.70	m
system volume		$5.34 \cdot 10^{-3}$	m^3
nominal CO_2 charge		2.945	kg

Table 1 Overview of secondary cycle test rig dimensions

As being present in air with ≈ 0.04 Vol.%, CO_2 is non-toxic under normal conditions. However, high concentrations of CO_2 (>12 Vol.%) may lead to safety risks due to increasing toxicity, as e.g. investigated in [3] for passenger cars. Despite this intrinsic safety risk, even major leakage into the cabin is expected to be not as critical in combination with mandatory air exchange rates and large free cabin volume. Regarding Tab. 1, the charge for the investigated cooling point configuration should only lead to temporarily increased CO_2-concentration, yet to be investigated.
Considering state-of-the-art liquid coolants (as e.g. perfluoroethers), the system volume is estimated to be >15 l without excessive optimisation effort and at 3 times higher density.

2.4 Controller concept

Control of the primary and secondary cycle is performed according to Fig. 4 in separate SISO control loops to account for system modularity. At the cooling point, air outlet temperatures at the evaporators are controlled by mass flow variation via the mass flow control valves. In

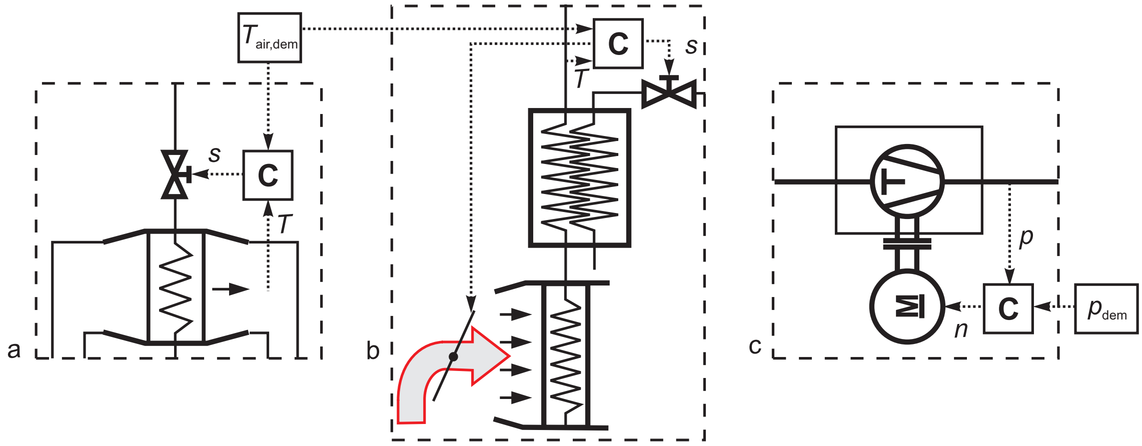

Fig. 4 Cooling system control loops: a) air temperature b) CO_2 supply temperature c) compressor discharge pressure (ground)

case of independent adjustment of demanded air temperatures, superheat control is reasonable to overcome strong cross coupling linked to fixed correlation of evaporation pressure and temperature in the 2-phase region.
At the CO_2-CO_2 Heat Exchanger or AHX, the supply temperature has to be controlled by the expansion valve or ram air mass flow, respectively.
The compressor discharge pressure in the primary cycle is controlled by the motor speed allowing process adaptation toward ambient temperature and total heat load as discussed in [2], [9]. Critical temperature and overpressure are thus monitored and limited.

3 Experimental Investigations of Ground Cases

3.1 Boundary Conditions

For on ground operation, high ambient temperatures are considered to estimate system sizing. In Fig. 5, a selection of steady state test results at constant ambient temperature of 30 °C, constant air flow rates and heat loads in the range of 1.1...1.7 kW (Evaporator E1) and 1.8...2.7 kW (Evaporator E3), respectively, are displayed. Successful tests at ambient air temperatures up to 48 °C were performed, where a reduction in cooling capacity has to be accepted (see [1]).

Noise variations as combined or individually changed heat loads, generation cycle discharge pressures and - over a wide range - control valve positions at E2 where applied to chart the system response. It is understood that for the actual applications, control of the cooling point air temperature has to be performed by individual or combined adjustment of the control valve and primary expansion valve (active primary cycle on ground) or ram air flow (direct condensation by ambient air during flight), respectively, as shown in Fig. 4. Here, the main focus lies on the system behaviour toward disturbances.

3.2 Test results

Qualitative examination of the results shown in Fig. 5 yield similar process diagrams. Compared to the idealised process in Fig. 3, pressure loss at the HX is higher (up to 1.23 bar) in relation to the evaporators. Merely pressure levels vary as the system is operated without closed loop control, leading to different cooling point air temperatures. These figures and other characteristic test data for the secondary cycle are given in Fig. 7.

Air temperatures vary from 0 to 14 °C, showing the system capability to adjust demanded temperatures, generally at 0...7 °C for galley cooling to prevent ice formation.
Inlet vapour qualities at the secondary cycle

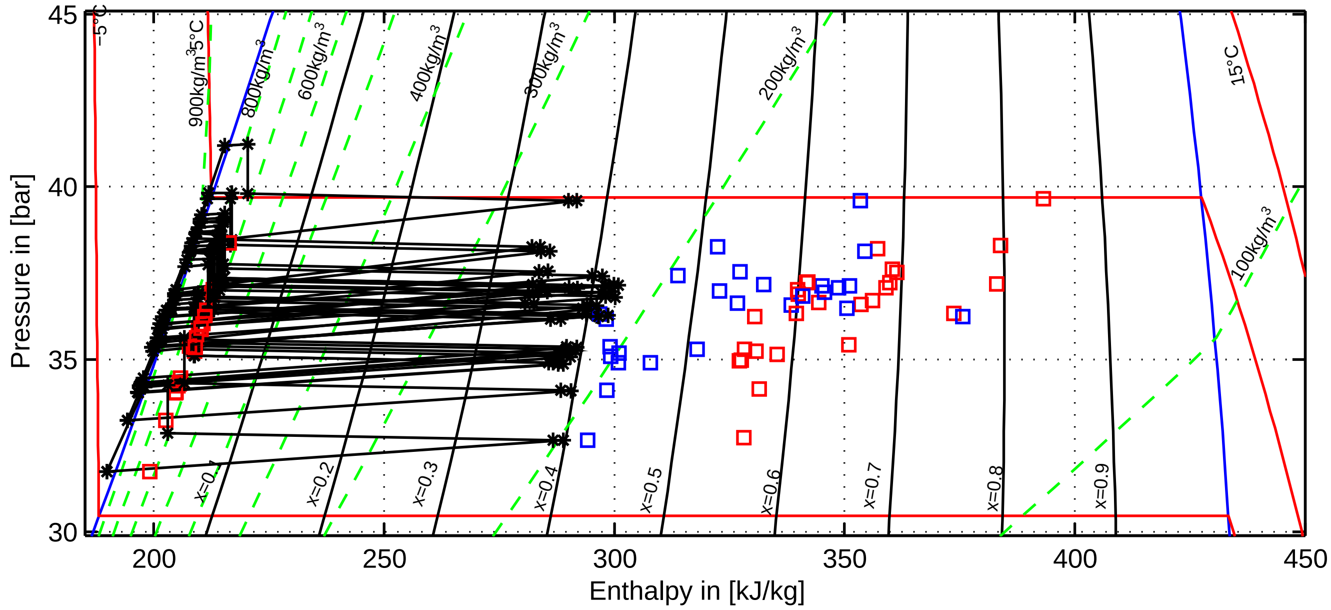

Fig. 5 Coolant cycle processes in *p*-*h*-diagram for varying evaporation temperatures; evaporator E1 (blue squares) and evaporator E2 (red) outlet states

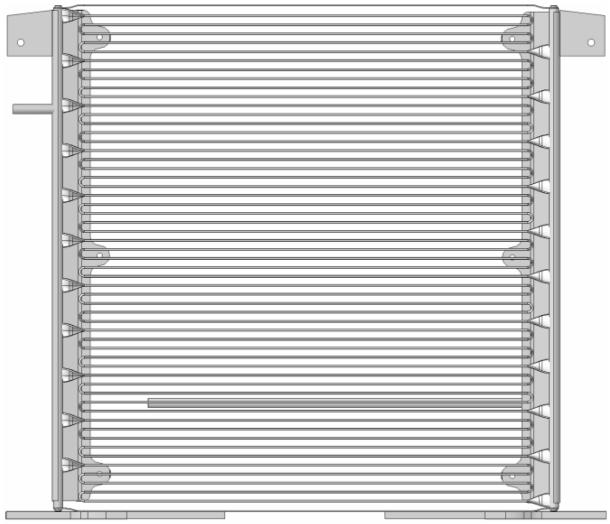

Fig. 6 Ambient heat exchanger (AHX, front view)

heat sink, previously determined as crucial for the achievement of sufficient condensation, are below 0.45 for all cases with a maximum CO_2 mass flow rate of 0.063 kg/s and 0.053 kg/s average mass flow. Regarding the evaporator outlet vapour qualities, even though values around 0.8 are reached at E2, mixture of both evaporator return mass flows with the bypass flow reduce vapour qualities significantly.

Pumping power with a differential pressure of $\Delta p_{Pump} = 2.3 \ldots 2.9$ bar varies at a pump capacity of 0.35...0.5 kW, leading to minor enthalpy increase from inlet to discharge (compare Fig. 5). This minimises both power consumption and heat gain. In order to yield the total pump power consumption, an additional constant power of 0.25 kW must be considered. Compared to state-of-the-art systems with single phase coolants, the pump capacity being equivalent to heat gain reaches up to 1.5 kW for identical cooling capacity.

4 Heat exchanger investigations

For ground operation, the interface between both partial systems is a CO_2-CO_2 counter flow heat exchanger. Its function is to transfer heat from the distribution cycle to the generation cycle and coolant condensation in the secondary part. This task is covered by the Ambient HX during cruise flight (compare Fig. 1).

The heat exchanger between the two loops is designed similarly to the internal heat exchanger in the primary cycle. Two counter flow HX of $d = 16$ mm outer diameter and $l = 1925$ mm length are passed through in parallel. These HX have been selected and designed to transfer a heat flux of up to 8 kW, depending on fluid states and

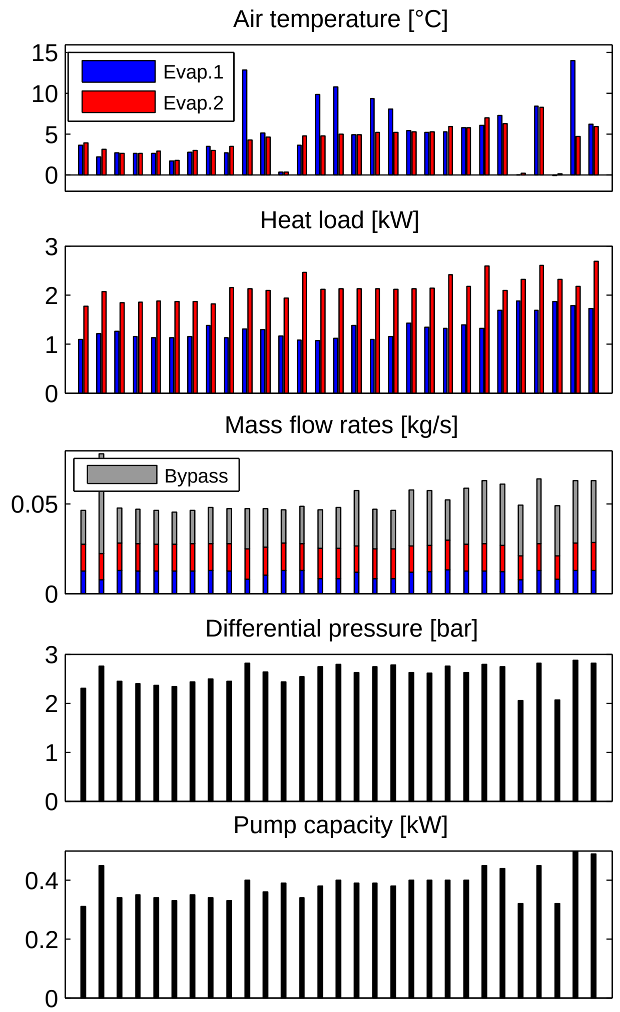

Fig. 7 Overview of CO_2 coolant cycle test results for 2 consumer ground operation at 30 °C ambient temperature

mass flows.
The evaporating, 2-phase refrigerant passes the outer sections, while the condensing 2-phase coolant passes through the smaller, inner pipe due to its higher density. This leads to minimised pressure loss along the HX:

- evaporation → 0.6…1.5 bar
- condensation → 0.4…1.2 bar.

The Ambient Heat Exchanger is represented by an automotive type cross flow minichannel condenser/gas cooler suited for CO_2 with a face area of 490×530 mm^2 and a depth of 20 mm in air flow direction with 5×11 flattubes, shown in Fig. 6. This HX has been selected from available components as best solution resulting from a trade off between minimum pressure loss and maximum heat transfer coefficient, dominantly effected by the flow velocity v on the coolant side, as the heat transfer coefficient

$$\alpha \sim \mathrm{Re}, \mathrm{Pr} \sim f\left(v, \eta, d, \lambda, c_p\right) \qquad (2)$$

is dependent on the REYNOLDS and PRANDTL number and thus fluid flow states as velocity v, viscosity η, density d, thermal conductivity λ and heat capacity c_p as a simplified approach for film condensation inside pipes [4]. On the air side, louver fins are applied for increased area of heat transfer and turbulence.

4.1 Simulation Models

Since the supply of liquid coolant at the pump inlet is essential, the behaviour of the introduced Ambient Heat Exchanger is investigated, to assess the feasibility of the described operating mode with the selected prototype. This is performed by numerical simulation using the model library ACLIB based on the THERMOFLUID library and herein defined heat exchanger model based on the simulation environment DYMOLA/MODELICA [8].
The used model incorporates a quadratic friction loss model for the condensing coolant being calibrated to a nominal pressure loss at a defined mass flow comprising a density correction to reflect density changes linked to condensation in the discretised model. Formulation of the condensation heat transfer is given by a simplified approach for the two phase region and laminar/turbulent calculation of the single heat transfer coefficient for single phase state with fluid state parameters calculated by the CO_2 model by Span and Wagner [10]. This is acceptable with respect to accuracy since air heat transfer is predominantly influencing the heat transmission coefficient of the assumed pipe heat transfer and allows for improved numeric behaviour of the model. This can easily becomes obvious with reference to the equation for the pipe heat trans-

mission coefficient

$$k_{AHX} = \frac{1}{A_n\left(\frac{1}{\alpha_{CO_2}A_1} + \frac{c_{geo}}{\lambda_{Wall}} + \frac{1}{\alpha_{air}A_2}\right)} \quad (3)$$

$$\text{with } c_{geo} = \frac{ln\left(d/(d-2s_{Wall})\right)}{2\pi L_{pipe}} \quad (4)$$

where A_n is the reference area and A_1 and A_2 are the areas of heat transfer for coolant and air, respectively, considering $\alpha_{CO_2}A_1 >> \alpha_{air}A_2$, in spite of the effective inner pipe area for the coolant being roughly 10 times smaller compared to the air side. Formulation of air to wall (lamella) heat transfer for a louver fin heat exchanger is implemented according to [6].

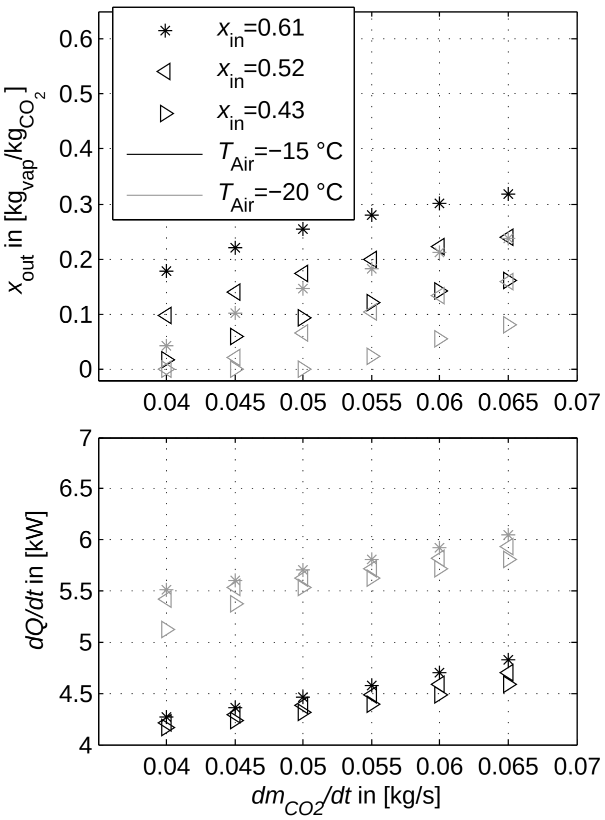

Fig. 8 Outlet vapour quality and heat flux at $p_{cond} = 35$ bar

4.2 Simulation Results

To assess the performance and applicability of the heat exchanger implemented at the test rig, parameter study results are discussed based on the diagrams shown in Fig. 8 to 10. This study is

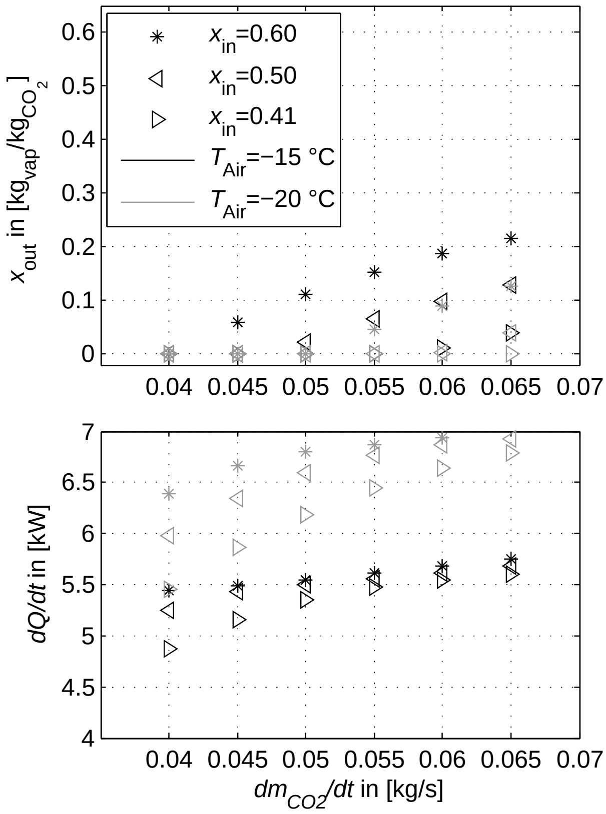

Fig. 9 Outlet vapour quality and heat flux at $p_{cond} = 40$ bar

also aiming at determination of operational limits regarding flight cases with direct condensation through ambient air. Herein, outlet vapour quality x_{out}, the transferred heat flux $\dot{Q}$ and the pressure loss Δp_{AHX} are shown for two different condensation pressure levels p_{cond} referring to relevant temperatures of 0 and 5 °C, varying ambient air temperatures T_{Air} and inlet vapour qualities x_{in}. All cases imply an air mass flow rate of $\dot{m}_{Air} = 0.4$ kg/s.

From the upper diagram in Fig. 8 and 9 it can be observed, that for maximum vapour qualities of ≈ 0.6, especially in combination with high mass flow rates $\dot{m} > 0.05$ kg/s, critical outlet vapour qualities ($x_{out} > 0.2$) are reached in certain cases, whereas incomplete condensation might lead to pump failure. This value is exceeded heavier at 35 bar compared to 40 bar, driven by a lower temperature difference to ambient air, also leading to minor transferable heat flux comparing the lower diagrams in Fig. 8 and 9. Taking the test results into consideration, 0.053 kg/s average

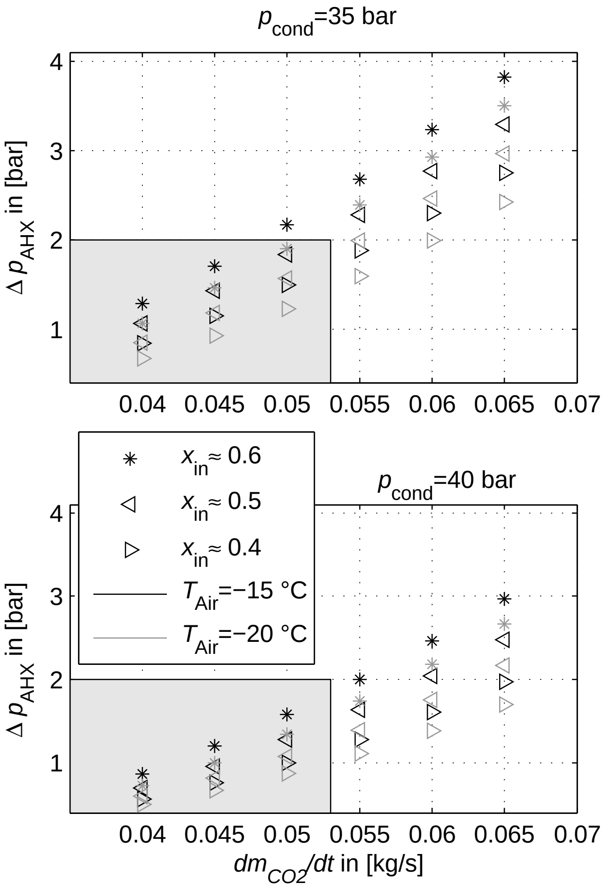

Fig. 10 Pressure loss at AHX for $p_{cond} = 35$ and 40 bar

mass flow and 0.42 maximum vapour quality are not critical regarding x_{out}. However, high inlet vapour qualities can be avoided by appropriate adjustment of the Bypass Valve.
To provide a minimum margin in cooling performance, $\dot{Q} = 5$ kW heat rejection is required for the intended application. Regarding the lower diagrams in Fig. 8 and 9, transferred heat $\dot{Q}$ is less dependent on vapour quality than mass flow rate, while higher values for x_{in} enable higher heat flux due to respective flow velocities. The results imply that an air temperature of ≤ -15 °C is required at $p_{cond} = 40$ bar and ≤ -20 °C at $p_{cond} = 35$ bar to transfer the required $\dot{Q} = 5$ kW, regarding the compact AHX.
Another important parameter is the pressure loss over the micro-tube AHX, influencing the pumping power and limiting the mass flow due to a low available differential pressure of $\Delta p_{Pump,max} \approx 4$ bar. A maximum pressure loss of ≈ 2 bar can thus be tolerated at the AHX. This limitation, together with the determined average mass flow rate of 0.053 kg/s, leads to the indicated operating range in Fig. 10 (gray box). With the previously identified constraints, all relevant points are within this operating range with a margin toward higher mass flow rates.

5 Conclusion and Outlook

In this paper, CO_2 is introduced as refrigerant and evaporating coolant in an on-board cooling system. Experimental results from an accordant test rig are used to demonstrate the capabilities and potential advantages of a 2-phase coolant regarding pumping power and heat transfer compared to liquid (single phase) coolants.
Based on the introduced results, the operational limit of the regarded AHX can be derived. A maximum mass flow rate of ≈ 0.055 kg/s in combination with a maximum inlet vapour quality at the AHX of 0.4 to 0.5 can be handled with respect to pump inlet vapour quality and rejected heat flux. With given AHX dimensions, condensation pressures of 35 and 40 bar are covered with the design air mass flow rate of 0.4 kg/s.
As a general statement, simulation results show sufficient condensation under most operating conditions. High inlet vapour qualities can be avoided by appropriate adjustment of the Bypass Valve. Considering maximum required mass flow rates of $\dot{m} < 0.02$ kg/s for maximum heat loads at each evaporator point out the fact, that the shown results are covering worst case conditions. In addition, optimisation of the heat exchanger geometry for the targeted operating range is feasible without major size increase. This allows either decrease of ram air mass flow causing aircraft drag or increased heat flux.
For validation of the concept for direct condensation through ambient air, the test rig is currently being modified to allow investigation of flight cases. Thus, the primary cycle is utilised for cold air generation circulated in a closed loop to simulate ram air conditions in flight. Pressure

loss and heat transfer behaviour are in the main focus of investigations regarding the AHX.

Control of air and coolant supply temperature will be optimised to complete the system controller including transient operation between ground and flight case, incorporating the identified operational limits.

As a final statement, based on the introduced results, direct condensation of a 2-phase coolant is feasible for flight cases without active cooling by a vapour cycle. Potential benefits of this approach regarding power consumption during flight and increased vapour cycle availability per flight hour due to reduced operating time are expected.

Acknowledgements

The test rig used for experimental investigations was set up with support from various companies, explicitly naming *Hermetic Pumpen GmbH* and *Eaton Aeroquip* who assisted in provision of components for the secondary cycle. As basis for the theoretical AHX investigations, heat exchangers provided by *Behr GmbH & Co. KG* were used.

Research on CO_2 in aircraft cooling system applications was performed in cooperation with *Airbus Deutschland GmbH* as part of the *AI-COOLS* project and the *Institute of Thermo-Fluid Dynamics* within the *Hamburg University of Technology*.

References

[1] Adeyefa S, Carl U, and Thielecke F. Concept of an indirect cooling system with co_2 als refrigerant and 2-phase coolant (in german). *Proc DKV-Tagungsband*, 2007.

[2] Adeyefa S, Schade O, and Carl U. Cop-optimised pressure control for a centralised co_2 cooling system in aircraft applications. *Proc 7th Gustav Lorentzen Conference on Natural Working Fluids*, Trondheim, Norway, May 2006. IIR.

[3] Amin J, Dienhart B, and Wertenbach J. Safety aspects of an a/c system with carbon dioxide as refrigerant. *Proc Automotive Alternate Refrigerants Systems Symposium Proc.*, 1999.

[4] Baehr H. D and Stephan K. *Wärme- und Stofübertragung*. Vol. 5. Auflage, Springer-Verlag Berlin Heidelberg, 2006.

[5] Cavallini A, Mannini A, Asinari P, and Zilio C. Carbon dioxide as a working fluid in aircraft air conditioning: an experimental assessment. *Proc IIR Conference 2005, Vicenza*, 2005.

[6] Chang Y and Wang C. A generalized heat transfer correlation for louver fin geometry. *International Journal of Heat Mass Transfer*, Vol. 40, No 3, pp 533 – 544, 1997.

[7] Fontelles J. B and Winkler H. Directive 2006/40/ec of the european parliament and of the council. *Official Journal of the European Union*, Vol. L161, pp 12–18, 2006.

[8] Pfafferott T and Schmitz G. Modeling and simulation of refrigeration systems with the natural refrigerant co2. *Proc 2nd International Modelica Conference*, pp 145–1 – 145–9, 2002.

[9] Schade O. *Theoretische und experimentelle Untersuchungen zur Prozessregelung von CO_2-Kälteanlagen mit parallelen Verbrauchern für Flugzeuge*. PhD thesis, Institut f. Flugzeug-Systemtechnik - Technische Universität Hamburg-Harburg, 2008.

[10] Span R and Wagner W. A new equation of state for carbon dioxide covering the fluid region from the triple-point temperature to 1100 k at pressures up to 800 mpa. *Journal of Physical and Chemical Reference Data (J.Phys.Chem.Ref. Data)*, Vol. 25, No 6, pp 1509–1596., 1996.

Copyright Statement